Conference Paper, Published Version

Medina, Josep; Gómez-Martín, M. Esther; Mares-Nasarre, Patricia; Odériz, Itxaso; Mendoza, Edgar; Silva, Rodolfo

Hydraulic Performance of Homogeneous Low-Crested Structures

Coastal Structures 2019 - Nils Goseberg, Torsten Schlurmann (eds) - © 2019 Bundesanstalt für Wasserbau
ISBN 978-3-939230-64-9 (Online) - DOI: 10.18451/978-3-939230-64-9_007

Hydraulic Performance of Homogeneous Low-Crested Structures

J. R. Medina, M. E. Gómez-Martín & P. Mares-Nasarre
Institute of Transport and Territory, Universitat Politècnica de València, Spain
I. Odériz, E. Mendoza & R. Silva
Instituto de Ingeniería, Universidad Nacional Autónoma de México, México

Abstract: Tourism activities associated with sandy beaches are essential to the economy of many countries around the world. The stability of many tropical beaches depends on the health of adjacent coral reefs. The retreat and progressive degradation of coral reefs reflect the poor health of the world´s marine ecosystems and threaten the economy and marine biodiversity in many places. Coastline protection is one of the ecosystem services provided by coral reefs. This can be mimicked by homogeneous low-crested structures (HLCS), a new type of reef breakwater, which is composed of very large, stable units without core. It is believed that HLCS can protect beaches and favor the colonization of coral, in appropriate conditions, while having minimum visual impact and thus being of exceptional value in areas where tourism is an important economic activity. 2D small-scale physical tests were carried out to describe the hydraulic performance of 1-layer, 3-layer and 5-layer Cubipod HLCS. Simple formulas using the dimensionless crest freeboard are provided to estimate the hydraulic performance: transmitted, reflected and dissipated wave energy.

Keywords: low-crested structures, green infrastructure, wave transmission, hydraulic stability, Cubipod, marine ecosystems

1 Introduction

The short-term benefits offered by tourism mean that pressure is growing in the coastal regions of many countries and consequently many coastal ecosystems are experiencing progressive degradation. Climate change affects coastal vulnerability and ecosystems, which are linked in many complex ways (Lowe et al., 2011). Ecosystem loss is also produced by ocean acidification and by the projected increase in extreme wave climate, sea level rise, erosion and flooding (Silva, et al., 2016).

Climate change and other human activities (pollutants, inadequate fishing, accidents, etc.) are serious threats to the world's coral reefs. Coral reefs around the world have been retreating at a rate of 1% to 2% annually over the last four decades (see Rinkevich, 2014). The recent progressive degradation of coral reefs in the Caribbean, Australia and South-East Asia has been described by Mumby et al. (2007) who give a clear indication of the poor health of marine ecosystems and the serious threats facing marine biodiversity (see Jones et al., 2004). This degradation also threatens the stability of the beaches protected by these coral reefs (see Ferrario et al., 2014).

Ecosystem health demands active measures (see Rinkevich, 2005) and coastal solutions must aim to reinforce the adaptation or restoration of ecosystems and thus mitigate coastal vulnerability. Nature-based coastal protection schemes have gained popularity, in part due to the social, economic and technical benefits they present (Schoonees et al., 2019). Homogeneous low-crested structures (HLCS) are made of large rocks or pre-cast concrete elements similar to a LCS without core, can in some cases be seen as multi-purpose green infrastructure (see Silva et al., 2017). When used as a detached breakwater, an HLCS can protect the coastline in the same way as a conventional low crested structure (LCS), but minimizing the environmental impacts; the construction phase is relatively clean, if necessary, dismantling is easy and, in the event of changes in the environmental conditions, the

elements are re-useable. In the long-term, the elements of the HLCS offer a statically stable structure which can withstand extreme storm waves, different from dynamically stable reef breakwaters of medium sized rocks (see Ahrens, 1989).

In addition, HLCS are highly porous structures which have a range of different light intensities between the elements that favors local biodiversity (Sherrard et al., 2016) and increases their value as green infrastructure. Although HLCS mimic the wave energy control provided by a coral reef, to restore habitats and enhance ecosystem services further information is needed. One of the main drivers of ecosystem connectivity are the local hydrodynamics, as these determine the colonization of potential species. Therefore, the study of HLCS and their impacts on hydrodynamics must be understood from an ecological perspective.

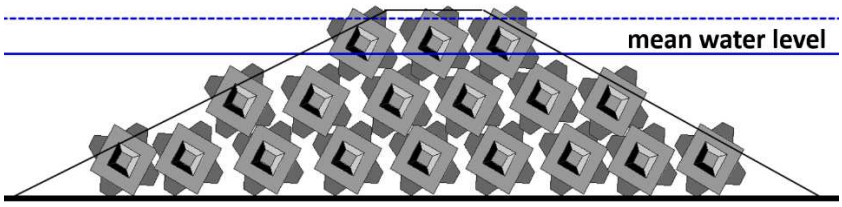

Fig. 1. Cross section of a typical 3-layer Cubipod HLCS. This is a statically-stable LCS without core which uses only one type of concrete armor unit (Cubipod) placed following specific placement grids.

The technical goal of this research was to design a HLCS able to withstand storm waves, and through small-scale experimental tests to evaluate wave transmission, dissipation and reflection for different storm waves and water levels. Once the hydraulic stability of the HLCS is established, being able to predict relative energy transmission and dissipation coefficients means that studies on connectivity and habitat adaptation evaluation can be conducted.

In this study, a new type of Cubipod HLCS was analyzed; it was seen to enhance certain ecosystem services and to facilitate marine ecosystem restoration. HLCS have considerable potential in the sustainable improvement of marine habitats (Odériz et al., 2018), which can subsequently serve as new points of touristic interest. Laboratory tests were carried out to analyze the comprehensive hydrodynamic response (transmitted, reflected and dissipated energy) of an HLCS that could enrich its surroundings ecologically and reduce coastal hazards there. Three structures were modelled: 1-layer (for the intertidal zone), 3-layers (subtidal zone), and 5-layers (subtidal zone). The experiments took place in the wave flume of the Port and Coastal Engineering Laboratory at the National Autonomous University of Mexico (UNAM). Placement grids, hydraulic stability and wave transmission, reflection and dissipation were analyzed. Simple formulas are given to estimate wave transmission, reflection and dissipation, based on the dimensionless crest freeboard.

2 2D Physical Tests

The porosity and hydraulic stability of an HLCS is highly dependent on the placement grids of concrete units. The first objective of this study was to find feasible placement grids for the 1-layer, 3-layer and 5-layer Cubipod HLCS. Section 2.1 describes the tests carried out prior to the experiments at UNAM and establishing the placement grid guidelines for a Cubipod HLCS.

Once the placement grids were defined, two series of 2D physical tests (scales 1/37.5 and 1/42.8) corresponding to structures A1 (1-layer), B5 (5-layer) and C3 (3-layer) and different water levels were conducted. The waves and foreshore conditions were selected to correspond to typical conditions in the Mexican Caribbean. Section 2.2 describes the experimental set up.

2.1 Placement grids

Medina and Gómez-Martín (2016) recommended diamond-type placement grids for Cubipod armored breakwaters. Cubipod HLCS, however, are qualitatively different from conventional Cubipod armors because the Cubipod units are placed in multiple horizontal layers. In this study, different rectangular- and triangular-type placement grids were considered and some of them were tested in the wave flume. The best results were obtained with the forward triangular-type placement grid shown in Fig. 2 where

the bottom layer is placed as usual (see Medina and Gómez-Martín, 2016) and each element of an upper layer is placed on three elements of the under layer (one on the seaward side and two on the leeside). Table 1 shows the geometric characteristics of feasible Cubipod placement grids for HLCS; the distance between the rows (e.g. a/D_{n50} =1.58 and b/D_{n50} =1.27) is referred to the nominal diameter or equivalent cube size of the units, D_{n50}.

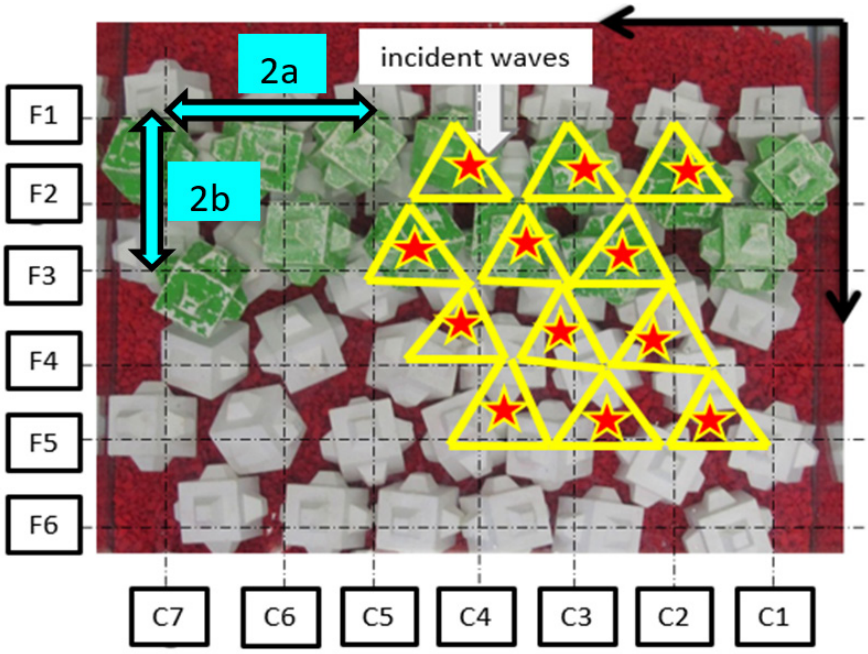

Fig. 2. Forward triangular-type placement grid for Cubipod HLCS placed on a diamond-type bottom grid. Each Cubipod placed in the second layer are supported on top of three Cubipod units from the bottom layer, one unit facing the incident waves and two units behind it.

Tab. 1. Geometric characteristics of feasible placement grid for Cubipod HLCS; distances between C-lines and F-lines define the basic rectangular grid for the placement of the bottom layer which may be either rectangular or diamond grid as shown in Fig. 2.

Line	Distance	Minimum Distance	Maximum Distance	Mean Distance
C	a/D_{n50}	1.31	1.84	1.58
F	b/D_{n50}	0.79	1.58	1.27

A number of preliminary hydraulic stability tests were conducted to select the best placement grids and the best structure configurations. It was observed that gentler frontal slopes have higher hydraulic stability. In this study, the forward triangular-type placement grid (see Tab. 1 and Fig. 2) was used to build up the Cubipod HLCS models tested in the wave flume. Once the placement grid was selected, three structures were designed for testing:

- HLCS-A1 (1-layer) with two rows of Cubipod units.
- HLCS-B5 (5-layer) with 11, 9, 7, 5 and 3 rows of Cubipod units; envelope slope H/V=1.5 seaside and leeside.
- HLCS-C3 (3-layer) with 9, 6 and 3 rows of Cubipod units; envelope slope H/V=2.0 and 1.5 seaside and leeside, respectively.

2.2 Experimental set up

The wave flume is 29 m long, 0.4 m wide and 0.52 m deep. Each HLCS model was placed on a horizontal platform elevated to 0.10 m above the bottom, with a m=2% bottom slope, the typical bottom slope of Caribbean beaches. Three wave gauges (WG2, WG3 and WG4) were placed in front of the HLCS, to measure the incident and reflected waves, following the approach of Mansard & Funke (1980) modified by Baquerizo et al. (1997), and three wave gauges (WG6, WG7 and WG8) were placed behind the HLCS, to measure wave transmission. A passive absorption gravel beach was

placed at the end of the flume and wave gauges were placed near the wave paddle (WG1) and the top of the HLCS model (WG5), respectively. Fig. 3 shows the experimental set up.

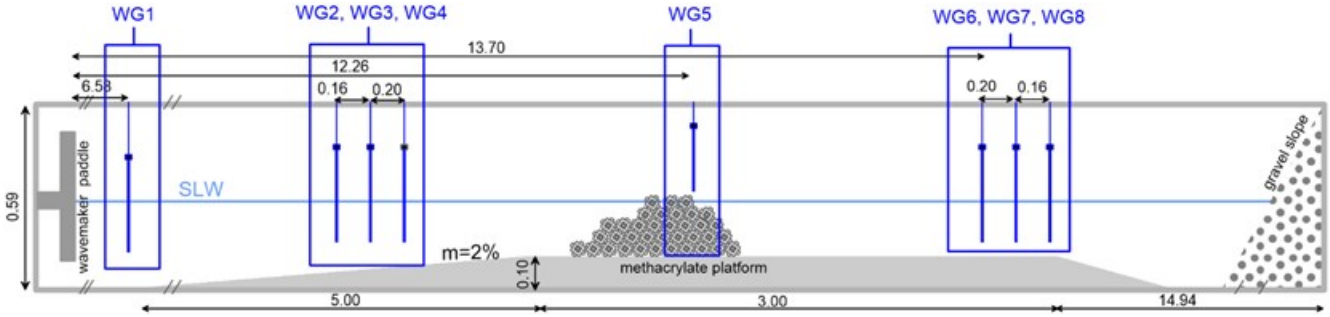

Fig. 3. Longitudinal cross-section of the experiments carried out (dimensions in meters).

Models of HLCS-A1, HLCS-B5 and HLCS-C3 were tested at scales of 1/42.8 and 1/37.5. The Cubipod units used were of mass density 2,280 kg/m^3 with D_{n50}[m]=0.0380 and 0.0435, respectively. Table 2 shows the test matrix of these experiments; each test lasted 20 minutes (approximately two hours at prototype scale) with irregular wave trains (JONSWAP, γ=3.3) characterized by the incident significant wave height, peak period, and water level. Each structure was tested with three different water levels: high water level (H), medium water level (M) and low water level (L). Each water level was tested under three different wave energy conditions: high wave energy (H), medium wave energy (M) and low wave energy (L).

Table 2 shows the specific Test ID for each test, using letters and a number. A, B or C indicates the geometry of the HLCS, and the following number, 1, 3 or 5, indicates the number of layers of the Cubipod HLCS (in this study: A1, B5 and C3). The third letter, a or b, indicates the scale of the test, a being 1/42.8 and b being 1/37.5. The fourth capital letter ("H", "M" or "L") indicates the wave energy ("H" for high wave energy, "M" for medium wave energy, and "L" for low wave energy). Finally, the fifth capital letter ("H", "M" or "L") indicates the water level ("H" for high water level, "M" for medium water level, and "L" for low water level). Table 2 shows the incident significant wave height and incident peak period measured by wave gauges WG2 to WG4, using the method to separate incident and reflected waves of Baquerizo et al. (1997). R_c is the crest freeboard of the structure.

Tab. 2. Test matrix.

Test ID	H_{si} (m)	T_{pi}(s)	R_c(m)	Test ID	H_{si} (m)	T_{pi}(s)	R_c(m)	Test ID	H_{si}(m)	T_{pi}(s)	R_c(m)
A1aLH	0.019	1.28	0.000	B5aLH	0.045	1.17	0.020	C3aLH	0.047	1.28	0.020
A1aLM	0.019	1.28	-0.010	B5aLM	0.044	1.17	0.010	C3aLM	0.046	1.28	0.010
A1aLL	0.019	1.28	-0.020	B5aLL	0.049	1.28	0.000	C3aLL	0.044	1.28	0.000
A1aMH	0.037	1.71	0.000	B5aMH	0.085	1.48	0.020	C3aMH	0.066	1.71	0.020
A1aMM	0.042	1.71	-0.020	B5aMM	0.087	1.48	0.000	C3aMM	0.066	1.71	0.000
A1aML	0.039	1.48	-0.050	B5aML	0.083	1.48	-0.030	C3aML	0.069	1.48	-0.030
A1aHH	0.044	2.06	0.000	B5aHH	0.093	1.76	0.020	C3aHH	0.066	2.06	0.020
A1aHM	0.055	1.94	-0.020	B5aHM	0.095	1.76	0.000	C3aHM	0.073	1.78	0.000
A1aHL	0.063	1.94	-0.050	B5aHL	0.098	1.76	-0.030	C3aHL	0.085	1.81	-0.030
A1bLH	0.029	1.26	-0.010	B5bLH	0.045	1.27	0.040	C3bLH	0.047	1.26	0.030
A1bLM	0.030	1.26	-0.020	B5bLM	0.050	1.27	0.030	C3bLM	0.048	1.26	0.020
A1bLL	0.029	1.26	-0.040	B5bLL	0.049	1.27	0.010	C3bLL	0.047	1.26	0.010
A1bMH	0.041	1.58	-0.010	B5bMH	0.098	1.63	0.040	C3bMH	0.072	1.62	0.030
A1bMM	0.043	1.56	-0.040	B5bMM	0.099	1.71	0.010	C3bMM	0.075	1.62	0.010
A1bML	0.040	1.56	-0.060	B5bML	0.103	1.71	-0.010	C3bML	0.077	1.62	-0.030
A1bHH	0.050	2.09	-0.010	B5bHH	0.104	1.91	0.040	C3bHH	0.073	2.09	0.030
A1bHM	0.068	2.09	-0.040	B5bHM	0.103	1.91	0.010	C3bHM	0.076	2.19	0.010
A1bHL	0.074	2.09	-0.060	B5bHL	0.116	1.91	-0.010	C3bHL	0.095	2.09	-0.030

3 Analysis of results

The hydraulic stability and wave-structure interaction of HLCS-A1, HLCS-B5 and HLCS-C3 are described in a previous work by Odériz et al. (2018). Some units in the A1, B5 and C3 models moved slightly during the tests described in Table 2. The key factor for LCS functionality in protecting sandy beaches is wave transmission. Section 3.1 analyzes the wave transmission recorded in the 54 tests which were carried out. Complementary, simple formulas to estimate the coefficient of transmission of Cubipod HLCS A1, B5, and C3 are provided. Section 3.2 analyses the wave reflection and energy dissipation.

3.1 Wave transmission

d'Angremond et al. (1996) correlated the coefficient of transmission with the dimensionless crest freeboard (R_c/H_{si}) and other explanatory variables (the dimensionless crest width and the Iribarren number) in their analysis of wave transmission for a conventional LCS, as in Eq. 1

$$C_t = -0.4\frac{R_c}{H_{si}} + 0.64\left(\frac{B}{H_{si}}\right)^{-0.31}\left(1 - e^{-I_{rpi}/2}\right) \quad (1)$$

where C_t = coefficient of transmission, R_c = crest freeboard, H_{si} = incident significant wave height, B = crest width, and I_{rpi} = Iribarren number considering H_{si} and peak period.

In this study, HLCS were seen to be more permeable than conventional LCS and the transmission coefficients measured are higher than those predicted by Eq. 1. Because of the reduced number of HLCS tests available, only the dimensionless crest freeboard was selected to estimate the coefficient of transmission of Cubipod HLCS A1, B5, and C3.

The transmission coefficients measured (C_t) from the 18 tests of Cubipod HLCS-A1 and 18 tests of Cubipod HLCS-C3, described in Table 2, were used to calibrate the formulas given by Eqs. 2 and 3 to estimate the transmission coefficients, C_t, of (A1) and C_t of (C3), respectively.

$$C_t(A1) = 0.45 - 0.30\left(\frac{R_c}{H_{si}}\right) \quad (2)$$

$$C_t(C3) = 0.60 - 0.35\left(\frac{R_c}{H_{si}}\right) \quad (3)$$

Eqs. 2 and 3 are valid for the ranges $-1.47 \leq R_c/H_{si} \leq 0.0$ and $-0.43 \leq R_c/H_{si} \leq +0.63$, respectively. Finally, the transmission coefficients (C_t) measured for the 18 tests of Cubipod HLCS-B (5-layer), described in Table 2, were used to calibrate the formula given by Eq. 4 to estimate the transmission coefficient C_t(B5).

$$C_t(B5) = max\left[0.54; 0.54 - 0.40\left(\frac{R_c}{H_{si}}\right)\right] \quad (4)$$

Eq. 4 is valid for the range: $-0.36 \leq R_c/H_{si} \leq +0.89$. Fig. 4 compares the measured and estimated transmission coefficients, using Eqs. 2 to 4. Fig. 4 shows the 5%, 50% and 95% percentiles of the estimated transmission coefficient (C_t); 90% confidence interval of estimations given by Eqs. 2 to 4 ranges ±0.08. Eqs. 2 to 4 can be used to estimate the transmission coefficients (C_t) of 1-layer, 3-layer and 5-layer Cubipod HLCS with only the dimensionless crest freeboard (R_c/H_{si}) as explanatory variable; the explained variance is more than 75%.

Fig. 5 compares the measured transmission coefficients C_t of Cubipod HLCS-A1, HLCS-B5 and HLCS-C3 with estimations given by Eq. 1 (LCS) and Eqs. 2 to 4. Eq. 1 proposed by d'Angremond et al. (1996) for conventional LCS estimate lower C_t than Eqs. 3 and 4 proposed for Cubipod HLCS-B5 and HLCS-C3, respectively. Eq. 1 estimate similar C_t than Eq. 2 proposed for Cubipod HLCS-A1, but two rows of Cubipod units (HLCS-A1 structure) is hard to be compared to a conventional LCS. As expected, wave transmission of conventional rock LCS with core is usually lower than Cubipod HLCS with similar envelope cross section.

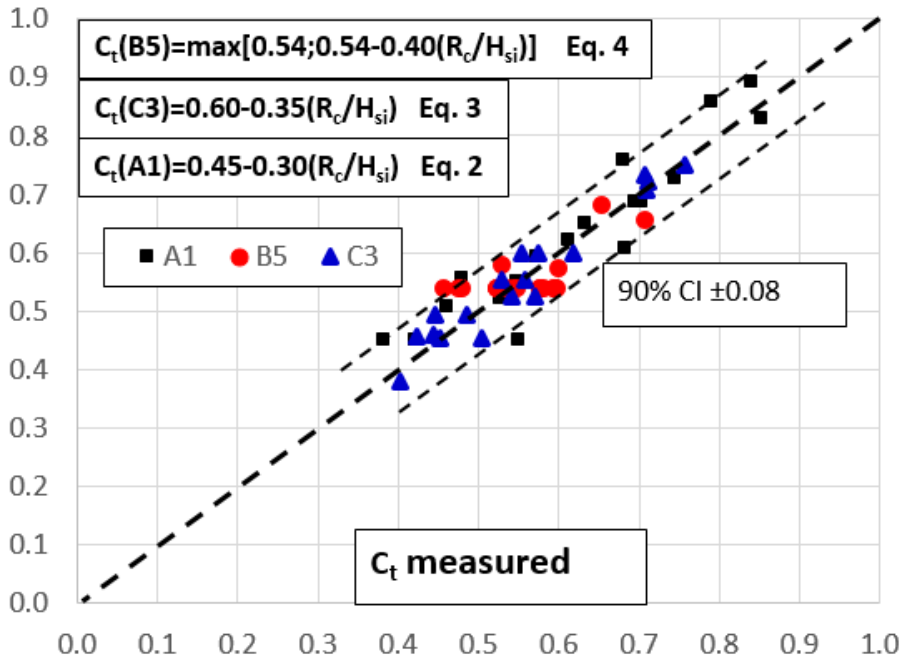

Fig. 4. Measured versus estimated transmission coefficient of Cubipod HLCS-A1, HLCS-C3, and HLCS-B5.

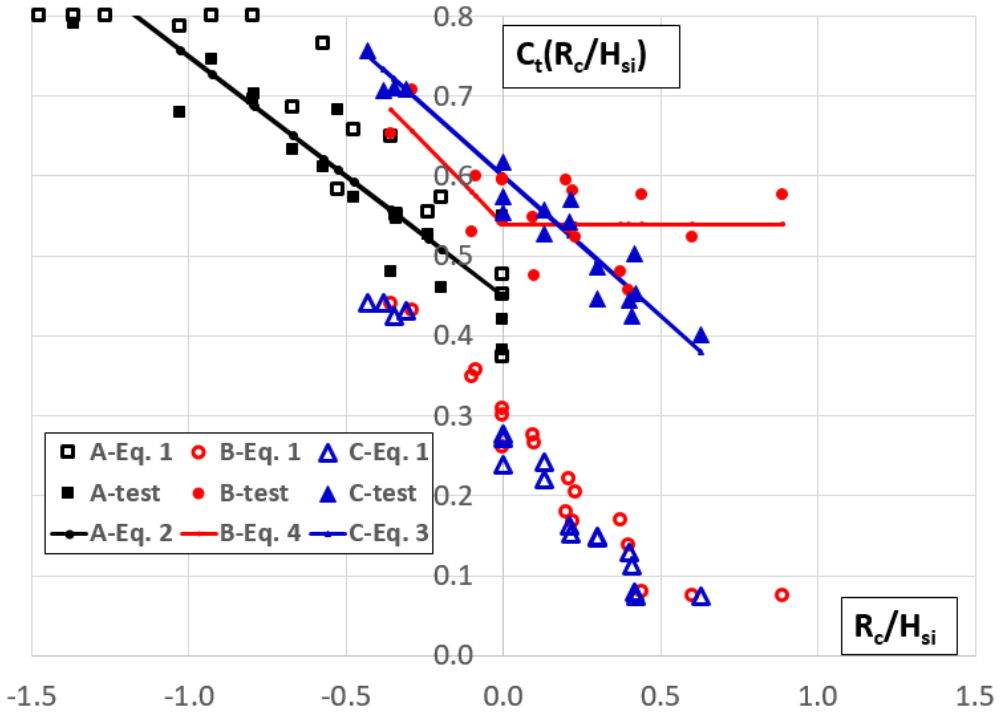

Fig. 5. Measured coefficient of transmission C_t (full symbols) of Cubipod HLCS-A1 (black), HLCS-B5 (red) and HLCS-C3 (blue) compared with estimated C_t given by Eq. 1 (open symbols) valid for conventional LCS and Eqs. 2 to 4 (lines).

3.2 Wave reflection and energy dissipation

The total wave energy (proportional to H_{si}^2) may be considered to be divided into three parts: transmitted wave energy (proportional to H_{st}^2), reflected wave energy (proportional to H_{sr}^2), and dissipated wave energy. Thus, the conservation of wave energy is proportional to $C_t^2=(H_{st}/H_{si})^2$, $C_r^2=(H_{sr}/H_{si})^2$, and C_d^2 according to Eq. 5.

$$C_t^2 + C_r^2 + C_d^2 = 1 \tag{5}$$

Incident, reflected and transmitted waves were separated using the 3-point method proposed by Baquerizo et al. (1997), using wave gauges WG2 to WG4 and WG6 to WG8 (see Fig. 3). The transmission coefficients (C_t) and reflection coefficients (C_r) were calculated for each test, and the proportion of dissipated wave energy was calculated using Eq. 5.

Fig. 6 shows the measured C_t^2, C_r^2, and the corresponding C_d^2=1-C_t^2-C_r^2, as a function of the dimensionless crest freeboard (R_c/H_{si}). The HLCS models studied show a trend similar to that of a conventional LCS; when the dimensionless crest freeboard (R_c/H_{si}) increases, wave reflection increases and wave transmission decreases. For dimensionless crest freeboards close to zero ($R_c/H_{is}\approx$ 0), the proportion of reflected, transmitted and dissipated wave energy is approximately 10% to 15%, 30% to 40%, and 50% to 60%, respectively.

The measured coefficients of reflection (C_r) from the 54 tests described in Table 2 were used to calibrate the formula given by Eq. 6, to estimate the reflection coefficient for Cubipod HLCS.

$$C_r = 0.36 + 0.05\left(\frac{R_c}{H_{si}}\right) \tag{6}$$

Eq. 6 is valid for the range: -1.47≤ R_c/H_{si} ≤0.89. Eq. 6 can be used to estimate the coefficient of reflection (C_r) of 1-layer, 3-layer and 5-layer Cubipod HLCS with the dimensionless crest freeboard (R_c/H_{si}) as the only explanatory variable; the explained variance is more than 25%.

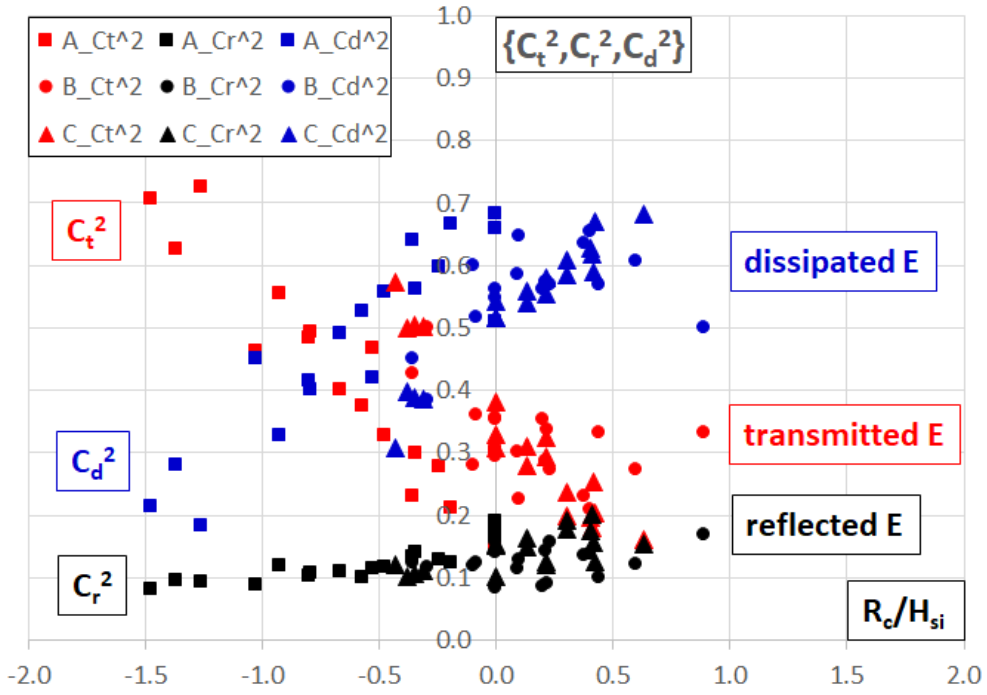

Fig. 6. Measured C_t^2 (red), C_r^2 (black) and C_d^2 (blue) as a function of the dimensionless crest freeboard (R_c/H_{si}) for Cubipod HLCS-A1 (squares), HLCS-B5 (circles) and HLCS-C3 (triangles).

Eqs. 2 to 6 can be used to estimate the proportion of reflected, transmitted and dissipated energy as a function of the dimensionless crest freeboard (R_c/H_{si}) for 1-layer, 3-layer and 5-layer Cubipod HLCS in the specified ranges of application.

HLCS and conventional LCS are usually designed as detached breakwaters, to reduce the incident wave energy arriving at the coastline. For a given incident wave energy at the toe of the structure, the performance (transmission coefficient) depends mainly on the crest freeboard. Given the design conditions and breakwater location, the incident significant wave height (H_{si}) and water level above the design water level (Δh) can be estimated, as well as the crest freeboard (R_c). Once the dimensionless crest freeboard (R_c/H_{si}) is calculated, Eqs. 2 to 6 can be used to evaluate the performance of Cubipod HLCS A1, B5 and C3.

Fig. 7 shows the proportions of incident wave energy which is reflected (C_r^2), transmitted (C_t^2) and dissipated (C_d^2) for a 3-layer Cubipod HLCS. The circles represent the measured values of C_r^2 (black), C_t^2 (red), and 1-C_t^2-C_r^2=C_d^2 (blue); the black, red and blue lines represent the estimated values using Eqs. 2 to 6.

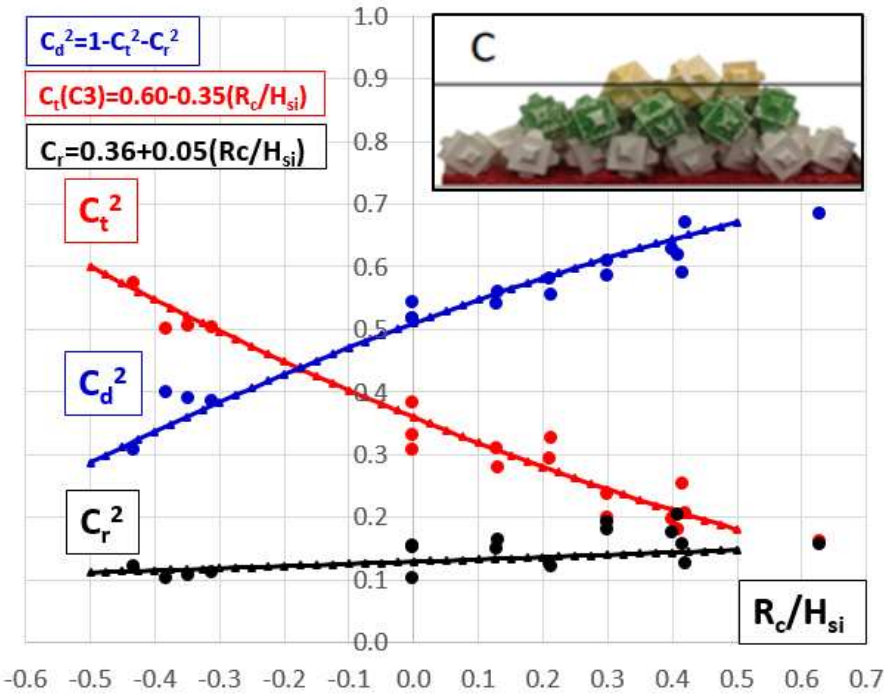

Fig. 7. Estimated and measured C_t^2, C_r^2, and C_d^2 for a 3-layer Cubipod HLCS (structure C).

4 Conclusions

The retreat of coral reefs threats the local economy and marine biodiversity in the Caribbean and many other places around the world where sea-sand-sun tourism is a key economic and social activity. One of the ecosystem services of coral reefs is coastline protection. In this study, a new type of LCS, called Homogeneous Low-Crested Structure (HLCS) is presented as a potential green infrastructure which may regenerate the retreating coral reef in the Caribbean and other areas of the world. The typical HLCS is made of only one type and size of a massive armor unit (e.g. cubes, Cubipods or large rocks) to form a LCS on a rocky sea bottom, which may be covered with a thin layer of sand.

HLCS used as detached breakwaters can protect the coastline and sandy beaches like a conventional LCS but minimizing the environmental impacts (clean construction, easy dismantling and re-useable units). HLCS are highly porous structures with heterogeneous illumination, which favors the colonization of a variety of marine species. In the long-term, the massive elements of HLCS offer a statically stable structure able to withstand extreme wave storms and, in the worst case, the structure can be easily dismantled and the elements re-used in other structures. In addition, HLCS may generate new points of touristic attraction because of the beauty of the marine species associated with artificial reefs (see Medina and Serra, 1987).

To assess the feasibility of the Cubipod HLCS in protecting a typical Caribbean beach, a study of placement grids and 2D physical tests for three structures (1-layer, 3-layer and 5-layer Cubipod HLCS) and two different scales (1/42.8 and 1/37.5) was carried out. Hydraulic stability depends on the placement grids; once these grids were selected (forward triangular-type placement grids), 1-layer (A1), 3-layer (C3), and 5-layer (B5) Cubipod HLCS were tested.

The coefficient of transmission (C_t), coefficient of reflection (C_r), and proportion of dissipated energy (C_d^2) can be estimated with Eqs. 2 to 6, which depend only on the dimensionless crest freeboard (R_c/H_{si}). As expected, HLCS show higher coefficients of transmission than conventional LCS, which have a relatively impermeable core, and wave transmission decreases when R_c/H_{si} increases. When the crest freeboard is null, the proportion of wave energy which is reflected, transmitted and dissipated is approximately 10% to 15%, 30% to 40%, and 50% to 60%, respectively.

The experimental work described here can be seen as a base for mimicking the hydraulic functions of a coral reef, thus recovering some of their ecosystem services; coastal protection and habitat provision for some species.

Acknowledgements

The authors wish to thank HUARIBE SA DE CV for funding this experimental research on HLCS and the financial support from European FEDER and Spanish *Ministerio de Ciencia, Innovación y Universidades* (Grant RTI2018-101073-B-100).

References

Ahrens, J.P., 1989. Stability of reef breakwaters. *Journal of Waterway, Port, Coastal, and Ocean Engineering,* ASCE, 115 (2), 221-234.

Baquerizo, A., Losada, M.A., Smith, J.M., Kobayashi, N., 1997. Cross-shore variation of wave reflection from beaches. Journal of Waterway, Port, Coastal, and Ocean Engineering, 123(5), 274-279.

d'Angremond, K., van der Meer, J.W., de Jong, R.J., 1996. Wave transmission at low crested structures. *Proc. of the 25th International Conference on Coastal Engineering,* ASCE, pp. 3305– 3318.

Ferrario, F., Beck, M.W., Storlazzi, C.D., Micheli, F., Shepard, C.C. Airoldi, L., 2014. The effectiveness of coral reefs for coastal hazard risk reduction and adaptation. *Nature Communications*, 5 (3794), 98-101.

Jones, G.P., McCormick, M.I., Srinivasan, M. Eagle, J.V., 2004. Coral decline threatens fish biodiversity in marine reserves. *Proceedings of the National Academy of Sciences of the USA*, 101(21), pp.8251-8253.

Lowe, J.A., Woodworth, P.L., Knutson, T., McDonald, R.E., McInnes, K.L., Woth, K., von Storch, H., Wolf, J., Swail, V., *et al*., 2011. Past and Future Changes in Extreme Sea Levels and Waves, in *Understanding Sea-Level Rise and Variability,* Eeds. J.A. Church, P.L. Woodworth, T. Aarup, and W. Stanley*, Wiley-Blackwell, UK,* 326–375.

Medina, J.R., Gómez-Martín, M.E., 2016. *Cubipod® Manual 2016*. Ed. Universitat Politècnica de València, 149 p. http://hdl.handle.net/10251/72310.

Medina, J.R., Serra, J., 1987. Arrecifes Artificiales (I). Problemas Pesqueros y de Protección de Costas. *Revista de Obras Públicas,* (Madrid), Nov. 1987, 725-735 (in Spanish).

Mumby, P.J., Hastings, A., Edwards, H.J., 2007. Thresholds and the resilience of Caribbean coral reefs. *Nature,* 450, 98–101.

Odériz, I., Mendoza, E., Silva, R., Medina, J.R., 2018. Hydraulic performance of a homogeneous Cubipod low-crested mound breakwater. *Proc. of the 7th International Conference on the Application of Physical Modelling in Coastal and Port Engineering and Science (Coastalab18)*, (in press).

Rinkevich, B., 2005. Conservation of coral reefs through active restoration measures: Recent approaches and last decade progress. *Environmental Science and Technology*, 39 (2005), 4333-4342.

Rinkevich, B., 2014. Rebuilding coral reefs: does active reef restoration lead to sustainable reefs? *Current Opinion in Environmental Sustainability*, 7 (2014), 28–36.

Schoonees, T., Gijón-Mancheño, A., Scheres, B., Bouma, T. J., Silva, R., Schlurmann, T., Schüttrumpf, H., 2019. Hard Structures for Coastal Protection, Towards Greener Designs. Estuaries and Coasts. https://doi.org/10.1007/s12237-019-00551-z.

Sherrard, T. R. W., Hawkins, S. J., Barfield, P., Kitou, M., Bray, S., Osborne, P. E., 2016. Hidden biodiversity in cryptic habitats provided by porous coastal defence structures. Coastal Engineering, 118, 12–20. https://doi.org/https://doi.org/10.1016/j.coastaleng.2016.08.005.

Silva, R., Lithgow, D., Esteves, L.S., Martínez, M.L., Moreno-Casasola, P., Martell, R., Pereira, P., Mendoza, E., Campos-Cascaredo, A., Grez, P.W., Osorio, A.F., Osorio-Cano, J.D., Rivillas, G.D., 2017. Coastal risk mitigation by green infrastructure in Latin America. *Proc. of the Institution of Civil Engineers-Maritime Engineering*, 170 (2), 39-54.

Silva, R., Mendoza, E., Mariño-Tapia, I., Martínez, M.L., Escalante, E., 2016. An artificial reef improves coastal protection and provides a base for coral recovery. *Journal of Coastal Research*, 75, 467-471.